Polymer Crystallization Kinetics: Poly(ethylene terephthalate) and Poly(phenylene sulfide)

K. RAVINDRANATH and J. P. JOG*

Chemical Engineering Division, National Chemical Laboratory, Pune 411008, India

SYNOPSIS

Analysis of isothermal crystallization data of PET and PPS was carried out using Avrami and Tobin models. The models gave fractional values of exponent n and the standard deviation varied between 1 and 4%. No improvement in the standard deviation could be obtained even after incorporating the nucleation rate in these models. The Hillier model gave a good fit only to the isothermal crystallization data of PET. A simple model considering primary and secondary crystallization has been proposed. The model is verified using isothermal crystallization data of PPS. © 1993 John Wiley & Sons, Inc.

INTRODUCTION

The mechanical and physical properties of the molded and extruded products of crystalline polymers are governed by the supermolecular morphology, which, in turn, is controlled by the crystallization process. In the processing of polymers, such as fiber spinning, injection molding, and extrusion, crystallization occurs under nonisothermal conditions.[1,2] Thus, nonisothermal studies are used to elucidate structure development in the melt processing of polymers and isothermal studies are used for investigating the mechanistic aspects of crystallization. The study of the kinetics of crystallization is necessary for optimizing the process conditions and establishing the structure–property correlations in polymers.

THEORETICAL BACKGROUND

Crystallization of polymers involves two consecutive processes: the formation of nuclei and their subsequent growth. When a polymer is supercooled by lowering its temperature below the polymer melting temperature (T_m), nuclei appear throughout the mass. The nuclei may appear instantaneously at the beginning of the process (heterogeneous nucleation) or they may appear in the untransformed phase throughout the process (homogeneous nucleation). The growth of the nuclei then occurs in one, two, or three dimensions, giving rise to rods, discs, or spheres. To describe quantitatively the macroscopic development of crystallinity in polymers, the following equation obtained from the classical theory of Avarmi for phase transformation kinetics is often applied[3,4]:

$$1 - X_t = \exp(-kt^n) \tag{1}$$

Here X_t is the degree of crystallinity; t, the time; k, the growth rate constant; and exponent n, represents the nucleation mechanism and growth dimensions. The value of n can be any positive integer between 1 and 4.

The Avrami model [eq. (1)] takes into account the formation of nuclei and their subsequent growth. However, in most of the cases, the experimental situation is complicated by different phenomena taking place during the course of crystallization and interpretation of the experimental data using the Avrami model leads to fractional values of the Avrami exponent (n) and deviations of the experimental data at longer crystallization times. These observations are generally attributed[5,6] to the simplified assumptions made in the Avrami model:

NCL communication number 5420.

* To whom correspondence should be addressed.

Journal of Applied Polymer Science, Vol. 49, 1395–1403 (1993)
© 1993 John Wiley & Sons, Inc. CCC 0021-8995/93/081395-09

- Constant radial growth rate
- Constant density and shape of the growing nuclei
- Uniqueness of the nucleation
- No secondary crystallization
- No volume change during phase transformation/crystallization.

Because of these assumptions, eq. (1) leads to fractional values of n that cannot be explained on any physical basis. Thus, many workers[5-10] developed models by relaxing one or several of the above assumptions. These models took into account a variable growth rate, a mixed mode of nucleation, a change in the density of the growing nuclei, the time dependence of the nucleation rate, and secondary crystallization. To explain the fractional values of n, Banks and Sharples[9] considered a mixed mode of nucleation where spherulitic growth occurs simultaneously from the nuclei originating instantaneously and sporadically with time. For a mixed mode of nucleation, eq. (1) can be rewritten as

$$1 - X_t = \exp(-k_1 t^n - k_2 t^{n+1}), \qquad (2)$$

where k_1 and k_2 are the two rate constants for heterogeneous and homogeneous nucleation, respectively. Equation (2) represents two processes occurring simultaneously with different integer values of n.

To improve the Avrami model, Tobin[6] proposed a new expression for growth site impingement and expressed X_t in terms of a nonlinear integral equation. The zeroth-order expression is given by

$$X_t/(1 - X_t) = kt^n \qquad (3)$$

A similar equation was proposed by Rabesiaka and Kovacs[12] and it was found to give a good fit to the experimental data for X_t up to 0.9. For small t, i.e., small values of X_t, eq. (3) approximates eq. (1) very well. At long times, however, X_t approaches unity faster in the case of the Avrami model compared with the Tobin model. Since experimental values deviate from the Avrami model at long times, Tobin considered it as positive evidence for his theory. However, Eder et al.[2] attributed the deviations at long times to the distribution in the activation times and not to the growth site impingement.

Aggarwal et al.[7] attributed the deviations of the experimental data from the values predicted using the Avrami equation to the secondary crystallization occurring within the spherulites. They assumed that the secondary crystallization proceeds as a first-order process. From the microscopic studies, they measured the number of spherulites as a function of time and found that the nucleation rate can also be represented by a first-order process:

$$N = N_0(1 - e^{t/tn}) \qquad (4)$$

where N_0 is the maximum number of nuclei at the end and t_n is the nucleation time constant. By taking into consideration these two factors, they have shown that the crystallization process can be described using four parameters, namely:

- time constant for primary crystallization
- time constant for secondary crystallization
- time constant for nucleation and extent of secondary crystallization.

The two-range equation considered by Danusso et al.[8] approximates eq. (4). Consideration of the nucleation rate in the Avrami theory leads to the following equation[7]:

$$\ln(1 - X_t) = -k'N \int_0^t (t - \theta)^n e^{-\theta/tn}\, d\theta \qquad (5)$$

Upon integration, one obtains

$$1 - X_t = \exp[-kf(t)] \qquad (6)$$

where

$$f(t) = t^2 - 2t_n t - 2t_n^2(e^{-t/tn} - 1) \quad \text{for} \quad n = 2 \qquad (7)$$

$$f(t) = t^3 - 3t_n t^2 + 6t_n^2 t + 6t_n^3(e^{-t/tn} - 1) \quad \text{for} \quad n = 3 \qquad (8)$$

Here, $k = k'N_0$. It is important to note that eq. (5) neglects the swallowing of potential nucleation sites by the growing spherulites. From eqs. (7) and (8), one obtains two well-known limiting cases: heterogeneous nucleation ($t \gg t_n$) and homogeneous nucleation ($t \ll t_n$).

Many workers[2,7,10,13] attributed the deviation at long times to the slow secondary crystallization process. Two types of secondary crystallization processes are envisaged. One is the secondary/post-Avarami crystallization due to the crystallization of the interspherulitic region. Another model proposed by Hillier[10] and Price[13] is the slow secondary crystallization occurring within a spherulite. In the Hil-

lier model, spherulites are assumed to grow at a constant rate and the volume occluded within a spherulite is given by the exponential form of eq. (1). Once a volume element is included in a spherulite, crystallinity is assumed to jump from zero to $X(p, \infty)$. Then, the slow secondary crystallization process occurs within the occluded volume and it is assumed to follow eq. (9):

$$X(s, t-\theta) = x(s, \infty)(1 - e^{-ks(t-\theta)}.) \quad (9)$$

Because of the secondary crystallization, density of the growing spherulite changes with time. The total crystallinity at time t is given by

$$X(t) = X(p, \infty)(1 - e^{kpt}) - X(s, \infty)k_s \int_0^t (1 - e^{-kp\theta})e^{-ks(t-\theta)}\, d\theta \quad (10)$$

$X(p, \infty)$ and $X(s, \infty)$ represent the total crystallinity due to primary and secondary crystallization, respectively. k_p and k_s are the rate constants for the primary and secondary processes, respectively.

All these models were found to give a good fit to the experimental data when compared with the Avrami model. But critical analysis of the experimental data using different models has not been undertaken yet. Therefore, in the present study, different models reported in the literature were used for checking their validity to isothermal crystallization of poly(ethylene terephthalate) (PET) and poly(phenylene sulfide) (PPS). Finally, a simple model taking into account primary and secondary crystallization is proposed in this work and it is verified using the isothermal crystallization data of PPS.

EXPERIMENTAL

The isothermal crystallization kinetics of PET and PPS were followed using a Perkin-Elmer DSC-2 differential scanning calorimeter equipped with a thermal analysis data station. The samples used for the present investigation were two grades of PET, namely, blow-molding grade (PETB) with intrinsic viscosity (IV) of 1.08 and injection-molding grade (PETI) with IV of 0.8 supplied by Cenka Plastics (India), and PPS supplied by Philips Petroleum (USA). The crystallization exotherms were obtained over a temperature range of 190–215°C for PET and 230–255°C for PPS. Before recording the exotherms, the samples were heated to 300°C and held at that temperature for 2 min to ensure complete melting of the polymer. The samples were then cooled at a rate of 160°C/min to a predetermined temperature (T_c) at which the exothermic crystallization peak was recorded. The extent of crystallization at any time was determined from point-by-point area measurements of the crystallization peak, assuming that the fractional crystallization at a given time is proportional to the ratio of the crystallization peak area up to that time to the total peak area. Results were reproducible and no noticeable degradation was observed during the experiments.

COMPUTATIONAL PROCEDURE

Marquard's nonlinear multivariable regression method[11] was used to analyze isothermal crystallization data of PETI, PETB, and PPS and to the various models examined in this work. Wherever analytical solutions are not possible, integrals were approximated using a 20-point Gauss quadrature formula. Marquard's method optimizes the parameters by minimizing the sum of squares of all deviations between the experimental and the calculated extent of crystallization. The standard deviation reported here is calculated from

$$\sigma = \sqrt{\frac{(X_{\text{cal}} - X_{\text{exp}})^2}{l - p}} \times 100$$

Here l is the number of data points and p is the number of model parameters.

RESULTS AND DISCUSSION

Figure 1 shows the isothermal crystallization data of PETI. The untransformed phase $(1 - X_t)$ is plotted against the logarithm of time at different crystallization temperatures (T_c). The observed characteristic sigmoidal shape of these isotherms is a very important feature of the crystallization process. There is an initial induction time (not shown in Fig. 1) followed by an accelerated crystallization process that reaches a pseudoequilibrium level of crystallinity depending on the T_c.

The solid lines in Figure 1 represent eq. (1) for $n = 2$ and $k = \ln 2/(t_{0.5})^n$ and it gives a good fit up to 70% conversion for all the isothermal crystallization temperatures considered in this work. It is well known that crystallization isotherms can be superimposed by shifting them along the time axis.

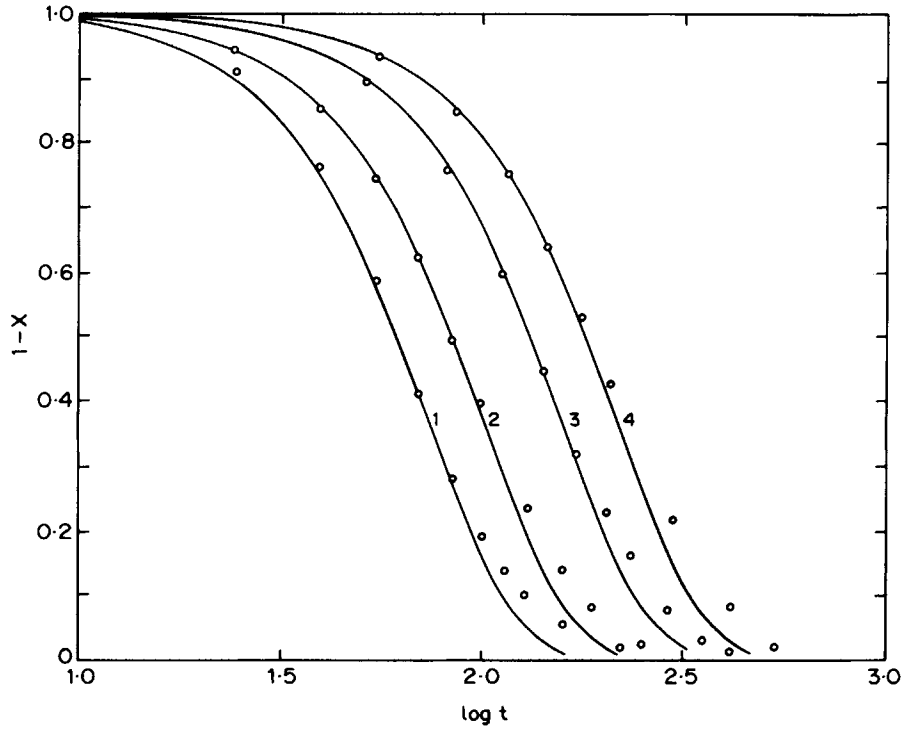

Figure 1 Amorphous fraction vs. time for PETI at different crystallization temperatures: (1) 190°C; (2) 195°C; (3) 200°C; (4) 210°C. Solid lines: eq. (1) and $n = 2$.

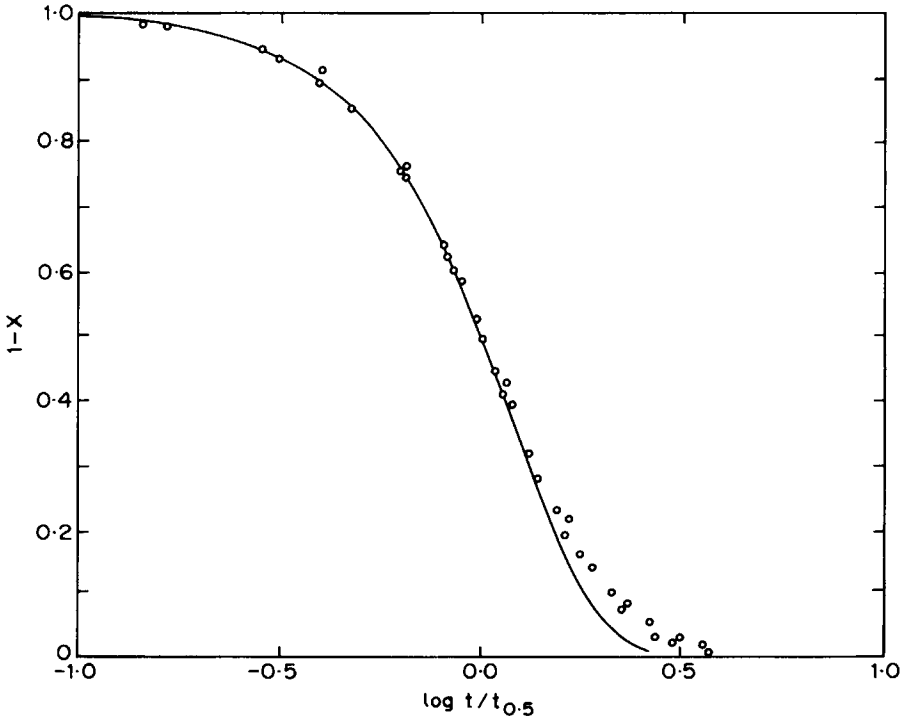

Figure 2 Amorphous fraction vs. reduced time for PETI at different crystallization temperatures (190, 195, 200, and 210°C). Solid line: eq. (2) and $n = 2$.

Superimposing of isotherms was done using $t_{0.5}$, viz., the time at which 50% of crystallization has taken place. Thus, eq. (1) reduces to

$$(1 - X_t) = \exp[-\ln 2(t/t_{0.5})^n] \qquad (11)$$

Equation (11) leads to a single master curve with a single reduced variable dependent on the temperature. Superposition of crystallization isotherms of PETI is shown in Figure 2 and the solid line in Figure 2 represents eq. (11) for $n = 2$. All isotherms collapse into a single curve, indicating that the crystallization mechanism is the same for all T_c's. Deviation from the Avrami theory is observed at above 70% conversion. Similarly, crystallization isotherms coalesce into a single master curve for PETB and PPS (see Figs. 3 and 4). Again, $n = 2$ gives a good fit up to 70% conversion for PETB. Therefore, a plausible structure is a fibrillar and/or lamellar growth of the polymer crystals. It is important to note that above 70% conversion PETB isotherms, unlike PETI and PPS, did not coalesce into a single curve, i.e., depending on the T_c, the crystallization mechanism changes at 70% conversion. Hence, eq. (2) cannot describe the complete crystallization process for PETB. In the case of PPS, a good fit could be obtained with $n = 2.5$.

Marquard's nonlinear regression method was applied to eq. (1) and optimum parameters of k and n were obtained. These are given in Table I for PETI, PETB, and PPS. The σ given in Table I represents the standard deviation and varies from 1 to 4%. As T_c increases, the crystallization rate is expected to decrease and the rate is zero when $T_c = T_m$. Hence, the growth rate constant, k, as shown in Table I, decreases as T_c increases. For all T_c's, fractional values of n were obtained. The value of n increases with T_c for PETI and PETB. However, no such trend is observed for PPS and the average value of n is 2.13.

Using eq. (2) proposed by Banks and Sharples[9] for a mixed mode of nucleation, the analysis of the experimental data did not result in either integer values of n or any improvement in the standard deviation. This is in agreement with Banks and Sharples' observation that eq. (2) could not give a good fit to their experimental data. In fact, the optimum value of k_2 obtained with the regression method is zero for most of the cases. When $k_2 = 0$, eq. (2) reduces to eq. (1).

The results of the analysis using eq. (3) proposed by Tobin[6] are tabulated in Table I. Even with the Tobin model, fractional values of n were obtained.

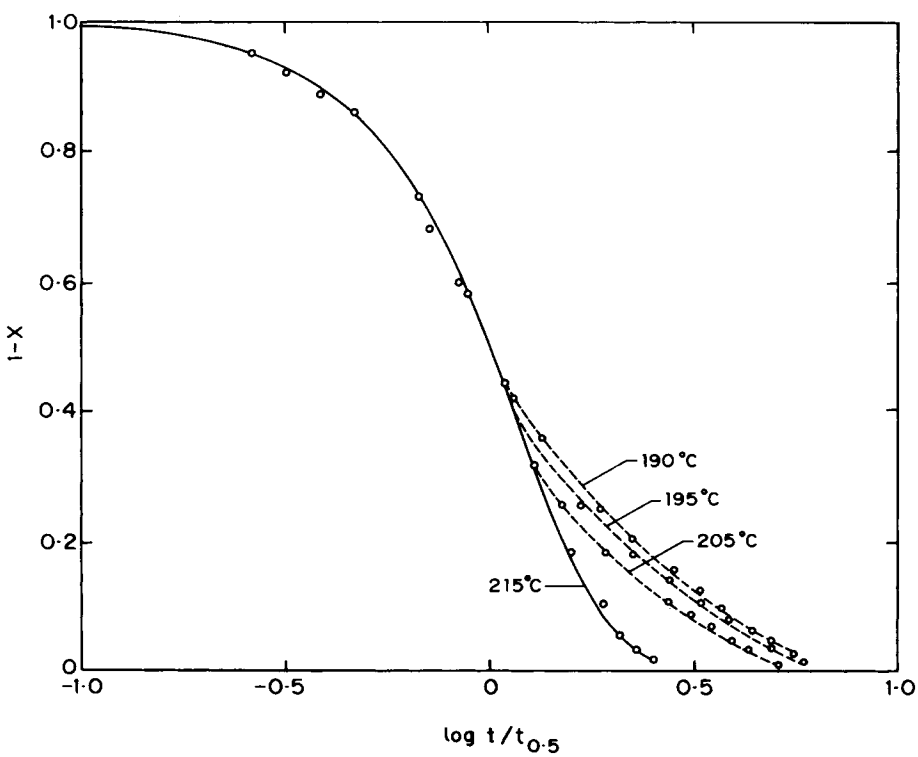

Figure 3 Amorphous fraction vs. reduced time for PETB at different crystallization temperatures (190, 195, 205, and 215°C). Solid line: eq. (2) and $n = 2$.

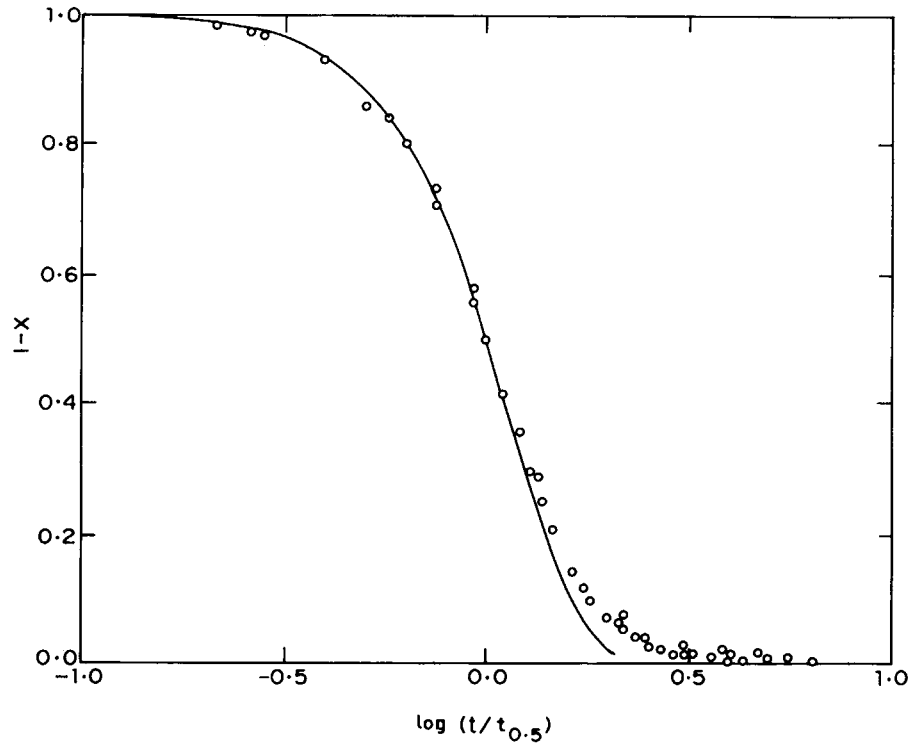

Figure 4 Amorphous fraction vs. reduced time for PPS at different crystallization temperatures (235, 245, 250, and 255°C). Solid line: eq. (2) and $n = 2.5$.

An important feature of the Tobin model is that the values of n were consistently greater than those obtained with the Avrami model and n varies between 1.8 and 3.45 (see Table I). For both models, the standard deviation is approximately same. However, there is a slight decrease in σ for PETB with the Tobin model.

Since the fractional values of n cannot be explained on any physical basis, many workers[7,10] developed models considering a variable growth rate, nucleation rate, and secondary crystallization. These models are used here for integer values of n. We shall now consider the effect of incorporating the nucleation rate in the Avrami and Tobin models.

Table I Crystallization Parameters Calculated Using Avrami and Tobin Models

		Avrami Model			Tobin Model		
Polymer	T_c	k	n	σ	k	n	σ
PETI	190	0.635	1.83	2.61	0.968	2.84	0.72
	195	0.371	1.76	1.42	0.434	2.65	1.80
	200	0.170	1.77	1.20	0.130	2.71	2.01
	210	0.093	1.76	1.13	0.058	2.59	2.08
PETB	190	0.392	1.11	3.73	0.427	1.84	1.73
	195	0.313	1.18	4.31	0.300	1.94	1.49
	205	0.201	1.33	3.98	0.143	2.18	1.97
	215	0.031	1.95	0.57	0.009	3.03	2.84
PPS	235	29.470	2.22	1.83	315.300	3.37	1.14
	245	4.210	2.01	1.92	16.300	3.01	1.46
	250	0.850	2.13	1.76	1.520	3.40	1.06
	255	0.170	2.17	1.60	0.130	3.43	1.45

Table II Crystallization Parameters Calculated Using Avrami and Tobin Models with Nucleation

	Avrami Model				Tobin Model		
Polymer	T_c	k	t_n	σ	k	t_n	σ
PETI	190	0.613	0.000	3.00	7.000	2.150	0.90
	195	0.325	0.000	2.79	1.740	1.120	2.27
	200	0.137	0.000	2.37	0.980	2.560	2.37
	210	0.071	0.000	2.53	0.300	1.820	2.60
PETB	190	0.195	0.000	9.55	0.368	0.000	2.29
	195	0.163	0.000	8.68	0.287	0.000	1.60
	205	0.097	0.000	6.46	0.212	0.000	1.00
	215	0.029	0.000	0.76	0.010[a]	0.000	2.85
PPS	235	26.200	0.024	1.66	23.400[a]	0.020	1.42
	245	4.400	0.011	1.88	16.200[a]	0.001	1.47
	250	0.990	0.077	1.59	2.420[a]	0.170	1.34
	255	0.240	0.196	1.44	0.290[a]	0.396	1.75

[a] $n = 3$.

Incorporating the nucleation rate in the Tobin model leads to the following simplified equation:

$$X_t/(1 - X_t) = kf(t) \tag{12}$$

$f(t)$ is given by eqs. (7) and (8) for $n = 2$ and 3, respectively. Marquard's regression method was applied to eqs. (6) and (9) for integer values of n. Table II shows the results. With the Avrami model, nucleation time is found to be zero for PETI and PETB. However, finite values of t_n were obtained for PETI and PPS with the Tobin model, but there is no particular trend in t_n values and the standard deviation did not improve even with the incorporation of the nucleation rate in the Avrami and Tobin models.

Considering the primary and secondary crystallization as discussed by Hillier,[10] the crystallization parameters were calculated and the results are presented in Table III. The standard deviation decreased for PETI and PETB and the average value of $X(p, \infty)$ is 0.45 and 0.64, respectively, for PETI and PETB. In fact, $X(p, \infty)$ is expected to increase with T_c, but no such trend was observed. It was observed that k_p, unlike k_s, is a strong function of temperature. The experimental data for PETB crystallized at 195°C is compared with the predicted values based on the Hillier model in Figure 5. Although the Hillier model could reduce the standard deviation for both the PET samples, in the case of PPS, consistent results could not be obtained with $n = 2$. Even with $n = 3$, σ did not improve and $X(p, \infty)$ of 0.255 (see Table III) is not expected for a fast crystallizing polymer such as PPS. It is probable that the Hillier model is not suitable for PPS.

As indicated earlier, the Hillier model takes into account only the secondary crystallization occurring within a spherulite and not the interspherulitic crystallization. Therefore, a simple model is proposed here considering inter- and intraspherulitic crystallization. The primary crystallization is assumed to follow

$$X_P = X_P(p, \infty)(1 - e^{-kptn}) \tag{13}$$

The mechanism of secondary crystallization can be described either by considering it as reorganization of the amorphous phase where crystallinity is linearly related to the logarithm of time or by considering it as a relaxation process where logarithm of

Table III Crystallization Parameters Calculated Using the Hillier Model

Polymer	T_c	k_p	k_s	$x\ (p,\infty)$	σ
PETI	190	0.809	0.821	0.817	1.21
($n = 2$)	195	0.687	0.992	0.450	0.35
	200	0.297	0.685	0.406	0.60
	210	0.144	0.452	0.447	0.78
PETB	190	0.672	0.353	0.537	0.85
($n = 2$)	195	0.394	0.282	0.620	0.41
	205	0.193	0.250	0.659	0.40
	215	0.036	0.417	0.747	0.40
PPS	235	331.000	9.670	0.266	1.30
($n = 3$)	245	44.500	3.800	0.203	2.07
	250	2.640	1.990	0.296	0.97
	255	0.310	1.000	0.255	1.17

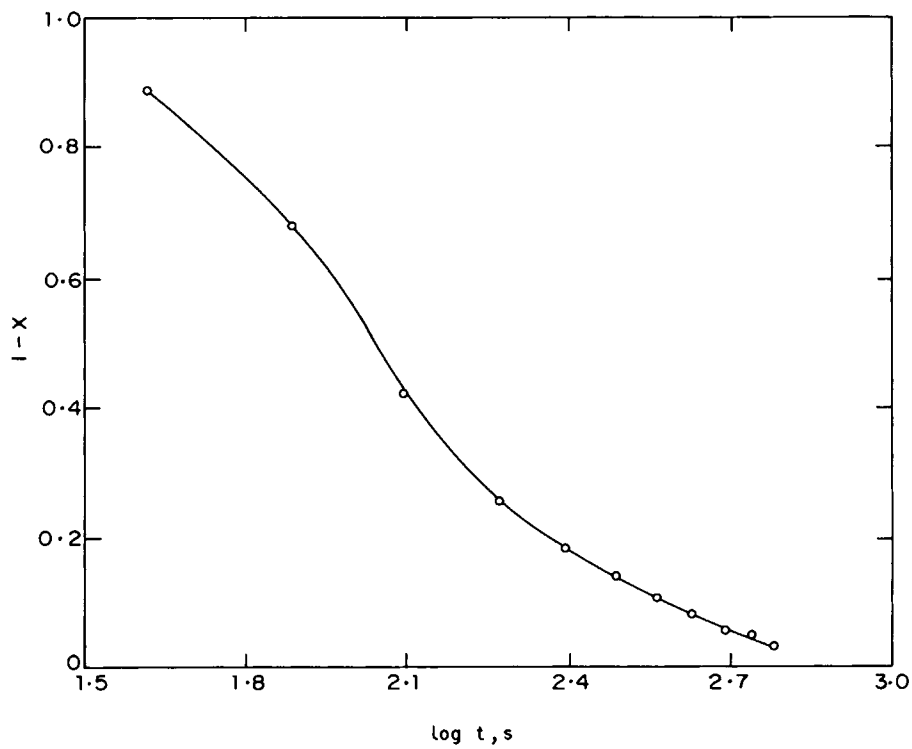

Figure 5 Comparison of the Hillier model predictions with the experimental data (PETB, T_c = 195°C).

crystallinity is linearly proportional to the time. However, experimental evidence suggests the latter mechanism.[14] Therefore, it is used here. Mathematically, it is represented by

$$X_s = X(s, \infty)[1 - e^{-ks(t-t_0)}] \quad (14)$$

Equation (14) represents the total secondary crystallization due to inter- and intraspherulitic crystallization and does not distinguish between these two processes. t_0 in eq. (14) is the time for the onset of secondary crystallization and it is not known *a priori* from DSC exotherms. However, Rybnikar[14,15] observed the onset of secondary crystallization by carrying out the experiments with dilatometry. By combining eqs. (13) and (14), we obtain

$$X_t = X(p, \infty)(1 - e^{-kptn}) + X(s, \infty)[1 - e^{-ks(t-t_0)}] \quad (15)$$

The main advantage of eq. (15) is that no integral has to be evaluated like in the Hillier model and it is simple to use even for nonisothermal studies. Table IV and Figure 6 show the results obtained with eq. (15) for PPS. The standard deviation decreases (see Table IV) compared with the Hillier model and $X(p, \infty)$ is 0.6. As expected, the time for the onset of secondary crystallization t_0 increases with T_c. It is important to note that t_0 is less than t_{peak} (time at which crystallization rate is maximum). It means that secondary crystallization starts before the crystallization rate reaches maximum. This is in contrast to Kamal and Chu's[4] assumption that secondary crystallization starts after t_p for polyethylene samples. This could be possibly due to different crystallization mechanisms of polyethylene and PPS. Further experiments are needed to verify the onset of secondary crystallization and to validate the proposed model in this work.

Table IV Crystallization Parameters for PPS Calculated Using the Proposed Model

Polymer	T_c	k_p	k_s	x (p,∞)	t_s (t_{peak})	σ
PPS	235	26.03	7.74	0.60	7.1 (10)	1.05
(n = 2)	245	6.01	2.90	0.66	17.7 (22)	0.66
	250	1.26	1.64	0.59	40.3 (50)	0.61
	255	0.24	0.83	0.64	74.5 (104)	0.66

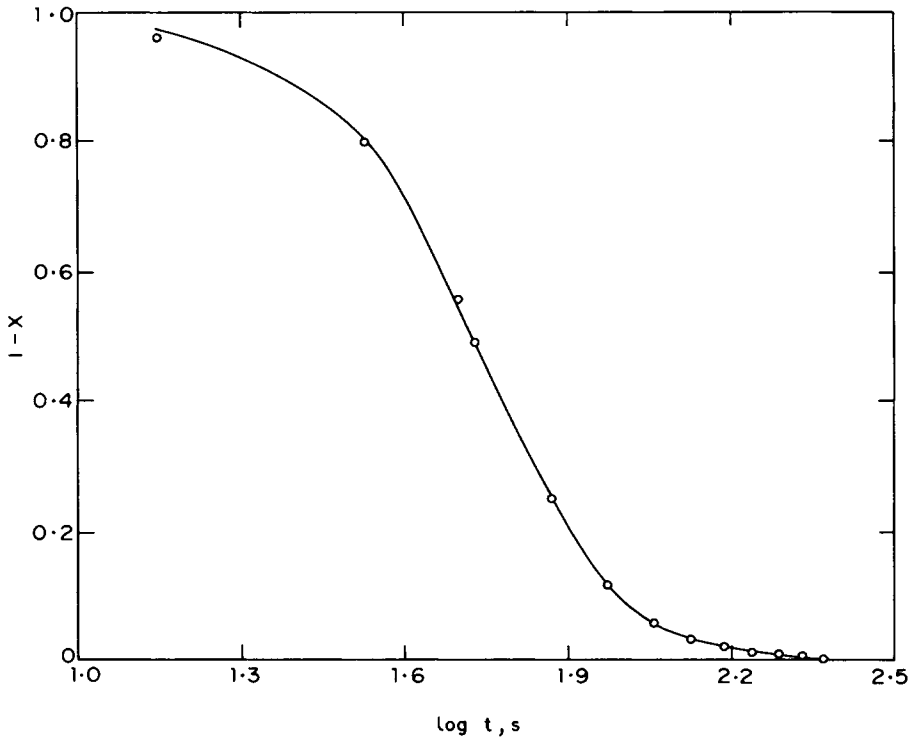

Figure 6 Comparison of proposed model predictions with the experimental data (PPS, T_c = 255°C).

CONCLUSIONS

Isothermal crystallization kinetics of PET and PPS was analyzed using the Avrami, Tobin, and Hillier models. Avrami and Tobin models gave fractional values of n and the value of n in the Tobin model was found to be greater than that obtained with the Avrami model. Even incorporation of nucleation rate in the Avrami and Tobin models did not reduce the standard deviation. The Hillier model was found to give good agreement for PETI and PETB. A simple model taking into account primary and intra- and interspherulitic crystallization was proposed. The model was tested with PPS and a good fit was obtained. The time for the onset of secondary crystallization is found to be less than t_{peak}. However, the proposed model did not give a good fit to PETI and PETB when compared with the Hillier model. Therefore, different models have to be employed to describe the crystallization mechanism of different polymers.

The authors wish to thank Dr. V. L. Shingankuli and Mrs. Bulakh for carrying out part of the experimental work.

REFERENCES

1. J. D. Muzzy, D. G. Bright, and G. H. Hoyos, *Polym. Eng. Sci.*, **18**, 437 (1978).
2. G. Eder, H. Janeschitz Kriegel, and S. Liedauer, *Prog. Polym. Sci.*, **15**, 629 (1990).
3. M. Avrami, *J. Chem. Phys.*, **7**, 1103 (1939); **8**, 212 (1940); **9**, 177 (1941).
4. M. R. Kamal and E. Chu, *Polym. Eng. Sci.*, **23**, 27 (1983).
5. S. P. Kim and S. C. Kim, *Polym. Eng. Sci.*, **30**, 110 (1990).
6. M. C. Tobin, *J. Polym. Sci. Polym. Phys. Ed.*, **12**, 399 (1974).
7. S. L. Aggarwal, L. Marker, W. L. Kollar, and R. Geroch, *J. Polym. Sci. A-2*, **4**, 715 (1966).
8. F. Danusso, G. Tieghi, and V. Felderer, *Eur. Polym. J.*, **6**, 1521 (1970).
9. W. Banks and A. Sharples, *J. Polym. Sci. Part A*, **2**, 4059 (1964).
10. I. H. Hillier, *J. Polym. Sci. Part A*, **3**, 3067 (1965).
11. J. L. Kuester and J. H. Mize, *Optimization Techniques with Fortran*, McGraw Hill, New York, 1973, pp. 240–250.
12. J. Rabesiaka and A. J. Kovacs, *J. Appl. Phys.*, **32**, 2314 (1961).
13. F. P. Price, *J. Polym. Sci. Part A*, **3**, 3079 (1965).
14. F. Rybnikar, *J. Polym. Sci.*, **44**, 517 (1960).
15. F. Rybnikar, *J. Polym. Sci. Part A*, **1**, 2031 (1963).

Received June 2, 1992
Accepted December 21, 1992